中國機械工程學刊第四十一卷第六期第 735~744 頁(民國一百零九年)
Journal of the Chinese Society of Mechanical Engineers, Vol.41, No.6, pp.735~744 (2020)

Automatically Tightening Tiny Screw to Cellphone with an Industry Robot

Jui-Chen Lu*, Pi-Cheng Tung **and An-Chen Lee***

Keywords： coordinate transformation, image processing, manipulator.

ABSTRACT

The objective of this research is to tighten tiny screws of the cellphone automatically by controlling a six-axis manipulator. The manipulator cooperates with two CCD cameras to perform initial positioning control and fine positioning control, respectively. One camera is fixed on a stationary frame above screw holes and the other is installed on the end effector of the manipulator. The captured images are processed and analyzed to detect the coordinate position of the screw holes. Through coordinate transformation and calculation, the hole positions of the space coordinate are found. A fine-tuning algorithm is developed to enhance the detection accuracy of hole position. Experimental results show that the proposed fine-tuning algorithm can tighten M1 and M1.1 screws into the target holes with the manipulator.

INTRODUCTION

Automation is a very popular research topic nowadays and within this trend, machine vision has been broadly used (Pérez et al., 2016; Jain et al, 2013). Using robots to replace the manual assembly becomes very popular. However, the assembly of cellphones is still relying on labor due to the fact that the size of most screws using in cellphone is less than M1.1. In machine vision applications for tightening screws, Pitipong et al. (2010) proposed a method of tightening a screw by using two cameras. The two cameras located at the same distance from the screw to take pictures from different sides of the screw. The purpose of image processing was to measure the angle of the screw, and to detect whether the screw is perpendicular to the screw hole. However, the accuracy of the coordinate position of the screw hole was not considered. The screw size was not discussed but apparently larger than that used in our research. Previous researches related to tightening tiny screws is also very limited. In this research, the cellphone screw is of M1.1 and M1. One CCD camera is set up above the cellphone and takes the entire cellphone picture. Initial positioning is performed to detect the position of all the screw holes to be tightened. The other is mounted on the end effector of the manipulator. When the manipulator moves directly above the target screw hole, the camera will only take a close-up photo of the screw hole for fine positioning.

Paper Received. Revised. Accepted. Author for Correspondence: Pi-Cheng Tung.
** Graduate Student, Department of Mechanical Engineering, National Central University, Taoyuan, Taiwan 32054, ROC.*

*** Professor, Department of Mechanical Engineering, National Central University, Taoyuan, Taiwan 32054, ROC.*

*** Professor, Department of Mechanical Engineering, National Chiao Tung University, Hsinchu, Taiwan 30010, ROC.*

The objective of the research is to develop a fine-tuning algorithm to increase the accuracy of screw hole detection. The human-machine interface (HMI) is design by Microsoft Visual Studio C++ for controlling the manipulator to tighten cellphone's screws. By clicking the buttons on the interface, a user can execute different commands, such as processing image, selecting objective screw hole, starting the manipulator, and starting the electric screwdriver, etc.

The image is processed by OpenCV to detect the coordinate positions of screw holes. The image processing methods used in the research are color model conversion, smoothing, morphology processing, adaptive thresholding, connected component, edge detection, and Hough circle detection. The position coordinate value of screw hole center based on imaging coordinate is obtained after image processing. The position coordinate value of screw hole center based on manipulator coordinate is obtained by performing coordinate transformation.

An electric screwdriver is modified and installed at the end effector of the manipulator for screw tightening. The screwdriver is activated through the HMI, and communicates with the Arduino microcontroller to perform different locking cycle time for different screw holes for completing the automatic screw tightening.

IMAGE PROCESSING

When two cameras take pictures of the cellphone's screw hole respectively, the picture should be processed in order to detect the position of screw hole center. In this study, the image is processed with OpenCV and the methods such as color model conversion (Nnolim, 2018), smoothing (Ma et.al, 2017; Sharmila, 2017), morphology processing (AhYin, 2011), adaptive thresholding, connected component (Gonzalez, 2007), edge detection (Bliton et.al, 1988), and Hough circle detection (Ballard, 1981; Tzvi, 1990; Bergen, 1991; Chen, 2000).

Color Model Conversion

The light source is one of controllable factors in this experiment. The values of RGB are converted to those of the HSV (Hue, Saturation, Value). The Hue (H) channel is adopted as a single channel to do the next process due to the fact that this approach gives better identification of objects in an image compared to those generated using RGB color space (Bora et.al, 2015).

Define (r, g, b) to be the value related to red, green, and blue coordinate of a color space respectively. The value is a real number between 0 and 1. Let max denote the largest among the three, and min denote the smallest of these three values. The conversion formula is:

$$h = \begin{cases} 0^\circ & if\ max = min \\ 60^\circ \times \frac{g-b}{max-min} + 0^\circ, & if\ max = r\ and\ g \geq b \\ 60^\circ \times \frac{g-b}{max-min} + 360^\circ, & if\ max = r\ and\ g < b \\ 60^\circ \times \frac{g-b}{max-min} + 120^\circ, & if\ max = g \\ 60^\circ \times \frac{g-b}{max-min} + 240^\circ, & if\ max = b \end{cases} \quad (1)$$

After conversion, the H channel is separated. For example, Figure 1 shows the processed result of a cellphone image.

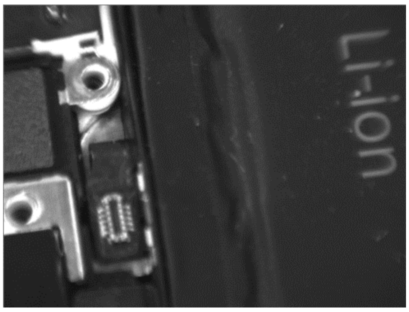

Fig. 1. H single channel image.

In the original image, the background is black and the edges of the target screw holes are white. In order to make the image more intuitive, the image is processed as a negative film at first. Figure 2 shows the processed result of a negative image.

Smoothing

To smooth image and reduce noise, in this paper, the initial positioning control uses Gaussian filter to perform image smoothing processing, and fine positioning control uses median filter.

Gaussian filter is a widely used linear filter. The formula of Gaussian filter is expressed as:

$$G_0(x,y) = A \cdot exp\left(\frac{-(x-\mu_x)^2}{2\sigma_x^2} + \frac{-(y-\mu_y)^2}{2\sigma_y^2}\right), \quad (2)$$

where A is the amplitude; x and y are the distance from the origin on the horizontal and vertical axis, and σ denotes standard deviation. Figure 3 shows a shape of the impulse response of a typical 2D Gaussian filter.

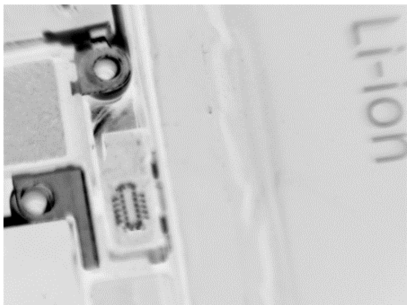

Fig. 2. Negative image.

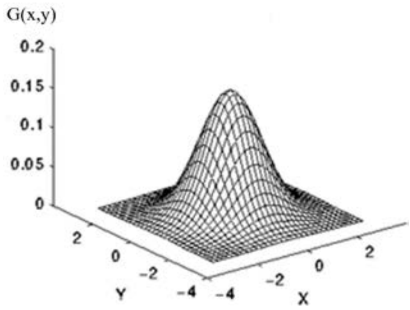

Fig. 3. Shape of the impulse response of a 2D Gaussian filter.

In this research, a 3 × 3 mask Gaussian spatial filter is used to smooth the image taken by camera 1. Figure 4 shows a cellphone image processed by a Gaussian filter.

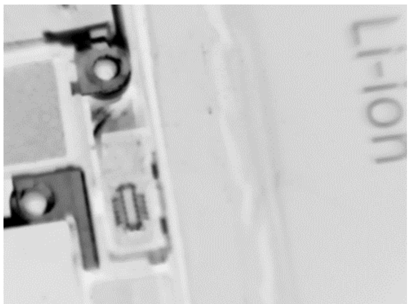

Fig. 4. Image processed by Gaussian filter.

The median filter is a non-linear filter. The pixel to be processed and its surrounding pixels are ranked according to the value of its gray scale. The processed pixel value is replaced by the ranked middle gray scale value.

The meaning of the median filter is to force the grayscale of the processed pixels to be similar to that of most of the surrounding pixels as possible. Therefore, the smoothing effect is significant, and the pixel noise of extreme difference values can be effectively eliminated.

In this research, a 3×3 mask median filter is used to smooth the image taken by camera 2. Figure 5 shows a cellphone image processed by the median filter. It is observed that the median filter removes noise while keeping edges relatively sharp and is suitable for fine tuning hole position.

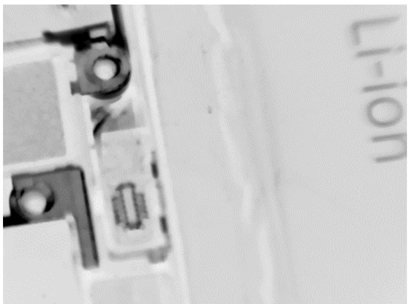

Fig. 5. Image processed by median filter.

Morphology Processing

Morphology operates as a mask in the operation of image processing. This mask is called a structural element. In this study, Dilation and Erosion are used a *3×3* mask to change the line thickness so that it can achieve better results in subsequent image processing.

Dilation: Amplify the gray scale set A with structural elements B (dilation of A by B), defined as:

$$A \oplus B = \max_{(i,j)\in B}\{a\,(x-i, y-j) + b(i,j)\}. \tag{3}$$

Erosion: Shrink the gray scale set A with structural element B (erosion of A by B), defined as:

$$A \ominus B = \min_{(i,j)\in B}\{a\,(x+i, y+j) - b(i,j)\}, \tag{4}$$

where $\ominus$ and $\oplus$ denote erosion and dilation, $a(x, y)$ and $b(i, j)$ are elements of the A, B set.

In mathematical morphology, opening is the dilation of the erosion of a set A by a structuring element B. Figure 6 shows the step of opening.

Fig. 6. Image processed by opening.

Adaptive thresholding

The selection of the threshold value of the adaptive threshold method (Gonzalez, 2007) to binarize an image is related to the grayscale of the image, the regional characteristics of each pixel, and the location of the pixel.

In this research, by using OpenCV, the optimal threshold is calculated with the mean and standard deviation. This method is also one of the most widely used calculation. Here we are choosing adaptive threshold of type binary and ADAPTIVE_THRESH_MEAN_C for threshold method. Figure 7 shows a cellphone image processed by adaptive thresholding.

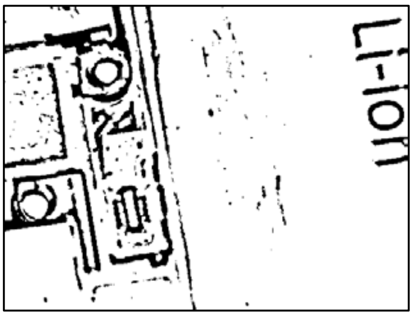

Fig. 7. Image processed by adaptive thresholding.

Connected Component (Gonzalez, 2007)

In the labeling method, labels are given to the same and similar gray scale pixels. Pixels with the same label can be connected into one component, called a connected component. The purpose of this step is to eliminate tiny noise and cellphone frame because both will lead to misjudgment of Hough circle detection.

The image is divided into front pixels and background pixels, and the pixels are judged twice in a left-to-right and top-to-bottom manner. Label is given to the pixel if it belongs front, and the label value is used to determine whether the corresponding pixels are connected. Figure 8 shows the steps of four connected components. The original image (left in Fig. 8) passes the first stage label (middle in Fig. 8) and the second stage label (right in Fig. 8). Figure 9 shows a cellphone image processed by four connected components.

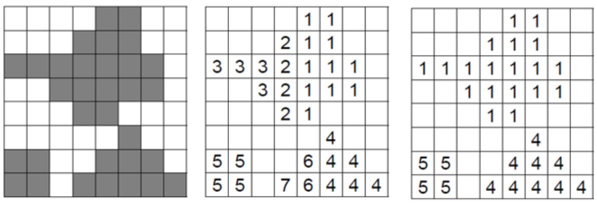

Fig. 8. Example of four connected components.

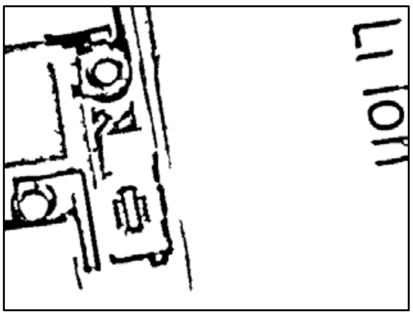

Fig. 9. Image processed by four connected components.

Edge Detection

Canny edge detection is used to identify contours in images. Many researches consider it as one of the best edge detection methods. The general criteria for edge detection are low error rate, accurate localizing, and a minimum response. Canny detection method (Bliton et al., 1988) mainly improves the edge detail and excludes unrelated features. This method is superior to other methods in terms of the quality of linearity, fineness, and continuity. In addition, the upper and lower thresholds of the canny edge detector are set to 50 and 150. The aperture size of the Sobel operator is set to 3. Figure 10 shows a cellphone image processed by Canny edge detection.

Fig. 10. Image processed by Canny edge detection.

Hough Circle Detection

Hough circle detection (Ballard, 1981; Tzvi, 1990; Bergen, 1991; Chen, 2000) is a widely used circle detection method. First, the position space needs to be converted into parameter space. Center coordinate is (C_1, C_2), C_3 is an unknown radius. The formula for the position and parameter space is expressed as:

Position space: $(x - C_1)^2 + (y - C_2)^2 = {C_3}^2$. (5)

Parameter space: $(C_1 - x)^2 + (C_2 - y)^2 = {C_3}^2$. (6)

The conversion process of position space to parameter space is shown in Figure 11.

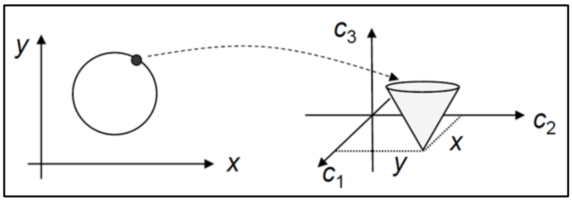

Fig. 11. Position space to parameter space.

For a circle detection, the more boundary points with the gradient direction we have, the better the method can detect whether the object is a circle or not. Figure 12 shows a cellphone image processed by Hough circle detection.

The circles detected by the Hough circle are the candidates. In these candidates, we need to define some rules to select the real screw holes. For example, choice any candidate to detect the grayscale value every 6 degrees on the circumference, and then we will obtain total 60 grayscale values. If more than 50 values are black, grayscale value is 255, this candidate will be retained. At the same time, we also incorporate the radius and center of the circle into the rules. Finally, the real screw holes will be screened out. Figure 13 shows a cellphone image processed by real screw holes detection.

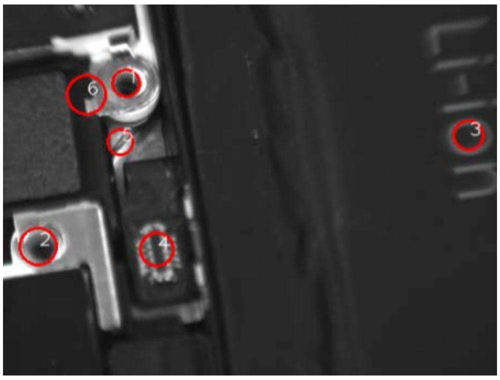

Fig. 12. Image processed by Hough circle detection.

Fig. 13. Image processed by Hough circle detection.

COORDINATE TRANSFORMATION

Applying the coordinate conversion method (Craig, 2008), the screw hole position coordinate obtained by image processing can be converted to the coordinate value of the manipulator.

Consider a point P and two coordinate systems $\{A\}$ and $\{B\}$.

${}^{A}P$: the point P in the coordinate system$\{A\}$.
${}^{B}P$: the point P in the coordinate system$\{B\}$.
$\hat{X}_A$: the unit vector of X direction in the coordinate system$\{A\}$.

Figure 14 shows rotation between the coordinate systems $\{A\}$ and $\{B\}$. $[{}^{A}\hat{X}_B \quad {}^{A}\hat{Y}_B \quad {}^{A}\hat{Z}_B]$ represents the unit vectors of $\{A\}$ relative to $\{B\}$.

$$
\begin{aligned}
{}^{A}_{B}R &= [{}^{A}\hat{X}_B \quad {}^{A}\hat{Y}_B \quad {}^{A}\hat{Z}_B] \\
&= \begin{bmatrix} \hat{X}_B \cdot \hat{X}_A & \hat{Y}_B \cdot \hat{X}_A & \hat{Z}_B \cdot \hat{X}_A \\ \hat{X}_B \cdot \hat{Y}_A & \hat{Y}_B \cdot \hat{Y}_A & \hat{Z}_B \cdot \hat{Y}_A \\ \hat{X}_B \cdot \hat{Z}_A & \hat{Y}_B \cdot \hat{Z}_A & \hat{Z}_B \cdot \hat{Z}_A \end{bmatrix} = \begin{bmatrix} r_{11} & r_{12} & r_{13} \\ r_{21} & r_{22} & r_{23} \\ r_{31} & r_{32} & r_{33} \end{bmatrix} \\
&= {}^{B}_{A}R'.
\end{aligned} \tag{7}
$$

The conversion equation between ${}^{A}P$ and ${}^{B}P$ is expressed as:

$$
{}^{A}P = {}^{A}_{B}R\,{}^{B}P. \tag{8}
$$

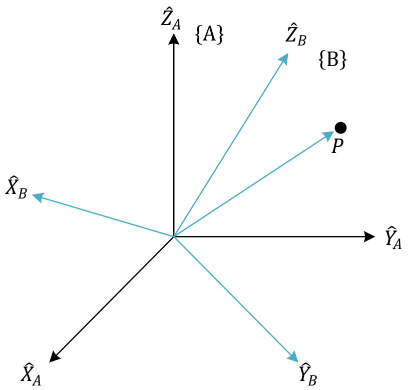

Fig. 14. Rotation between the coordinate systems $\{A\}$ and $\{B\}$.

Figure 15 shows the displacement and rotation between the coordinate systems $\{A\}$ and $\{B\}$. ${}^{A}P_{BORG}$ represents the origin displacement between $\{A\}$ and $\{B\}$. The conversion equation between ${}^{A}P$ and ${}^{B}P$ is expressed as:

$$ {}^{A}P = {}^{A}_{B}R\,{}^{B}P + {}^{A}P_{BORG}. \tag{9}$$

In order to clearly indicate the purpose of the coordinate system conversion, Equation (9) is rewritten as a 4 × 4 transformation matrix:

$$\begin{bmatrix} {}^{A}P \\ 1 \end{bmatrix} = \begin{bmatrix} {}^{A}_{B}R & {}^{A}P_{BORG} \\ 0 \quad 0 \quad 0 & 1 \end{bmatrix} \begin{bmatrix} {}^{B}P \\ 1 \end{bmatrix}. \tag{10}$$

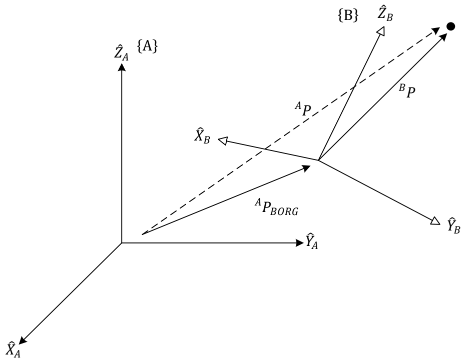

Fig. 15. The displacement and rotation between systems $\{A\}$ and $\{B\}$.

EXPERIMENT PLATFORM AND EQUIPMENT

The 6-DOF manipulator and camera 1 are fixed on the platform respectively as shown in Figure 16. Camera 1 is fixed above the cellphone. Camera 2 is installed on the end effector of the manipulator to take picture of the screw hole closely.

The resolution of camera 1 is 1280 × 960, and camera 2 is 1024 × 768. The focal length and aperture of the lenses are fixed during the experiment. Since the CCD camera is very sensitive to the light source, the light source is maintained by two lamps. A controller board Arduino UNO is used to control the DC motor of the electric screwdriver. A motor driver IC L298N is used to drive the motor and to tighten the screw. Some mechanisms are designed to fix the cameras. A permanent magnet attached to the head of the screw driver is used to stick the screws as shown in Figure 17. Table 1 shows the specifications of the experimental set-up.

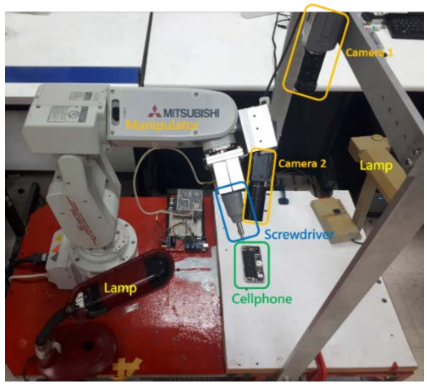

Fig. 16. The experiment platform.

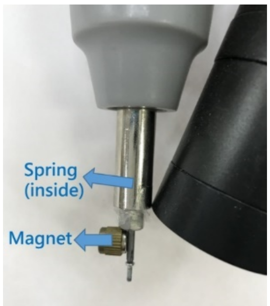

Fig. 17. Cellphone screw are attached to the screwdriver.

Table 1. Specifications of the experimental setup.

Equipment	Model/ Specification/Description
Manipulator	MITSUBISHI RV-2SD
CCD camera 1	SONY DFW-SX910
CD camera 2	SONY XCD-X710
Camera lenses	6~60 mm, F1.4
Image capture card	NI PCI-8254R
Microchip	Arduino UNO
Drive circuit	L298N
Electric screwdriver	Neopower 6V, 200 rpm
Screwdriver head	None
Screw	Disassembled from the cellphone
Cellphone	iPhone 5s

TRANSFORMATION EQUATION BETWEEN CAMERA 1 AND MANIPULATOR

The coordinate value of the screw hole center calculated by image processing needs to transform to the coordinate value of the manipulator by coordinate transformation. Therefore, the transformation equation between camera 1 and the manipulator needs to be calculated. Define $\{A\}$ to be the coordinate system of the manipulator, and $\{C\}$ to be the coordinate system of camera 1, as shown in Figure 18. The origin of $\{A\}$ is located in the center of the robot base, and the length unit is in mm. The origin of $\{C\}$ is located at the upper left corner of the image as shown in Figure 19. The length unit is in pixel.

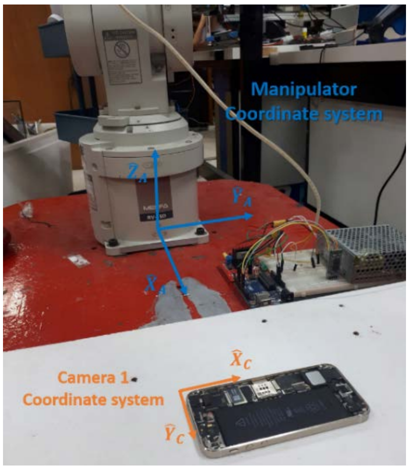

Fig. 18. The positions of the coordinate systems $\{A\}$ and $\{C\}$.

Fig. 19. The positions of the coordinate systems $\{A\}$ and $\{C\}$.

The Transformation Formula

The coordinate of the camera 1 can be converted by the following equations.

$$\begin{bmatrix} {}^{A}P \\ 1 \end{bmatrix} = \begin{bmatrix} {}^{A}_{C}R & {}^{A}P_{BORG} \\ 0 \;\; 0 \;\; 0 & 1 \end{bmatrix} \begin{bmatrix} {}^{C}P \\ 1 \end{bmatrix}. \tag{11}$$

$$\begin{bmatrix} X_A \\ Y_A \\ Z_A \\ 1 \end{bmatrix} = \begin{bmatrix} r_{11} & r_{12} & r_{13} & X_0 \\ r_{21} & r_{22} & r_{23} & Y_0 \\ r_{31} & r_{32} & r_{33} & Z_0 \\ 0 & 0 & 0 & 1 \end{bmatrix} \begin{bmatrix} X_C \\ Y_C \\ Z_C \\ 1 \end{bmatrix}. \tag{12}$$

${}^{A}P$: The coordinate value of the P point in the manipulator coordinate system, i.e. (X_A, Y_A, Z_A).

${}^{C}P$: The coordinate value of the P point in the Camera 1 coordinate system, i.e. (X_C, Y_C, Z_C).

${}^{A}_{C}R$: The rotation matrix between the two coordinate systems, consisting of $r_{11} \sim r_{33}$.

${}^{A}P_{CORG}$: The translation vector from the origin of camera 1 coordinate system to the origin of the manipulator coordinate system, i.e. (X_0, Y_0, Z_0).

The 4 × 4 transformation matrix consists of 12 unknowns needed to be calculated. Since the height of camera 1 is fixed, the objective Z_A can be set fixed, and Z_C is always 0. The formula can be simplified to the following equation, and there are 6 unknowns, $r_{11} \sim r_{22}$, X_0, Y_0 to be determined.

$$\begin{bmatrix} X_A \\ Y_A \\ 1 \end{bmatrix} = \begin{bmatrix} r_{11} & r_{12} & X_0 \\ r_{21} & r_{22} & Y_0 \\ 0 & 0 & 1 \end{bmatrix} \begin{bmatrix} X_C \\ Y_C \\ 1 \end{bmatrix}. \tag{13}$$

Measurement Data

At least 6 (X_A, Y_A) and (X_C, Y_C) data are needed to solve the 6 unknowns. Manually control the manipulator and align the screw at the screw holes vertically to get (X_A, Y_A) data. (X_C, Y_C) can be obtained by image processing. The measurement data is shown in Table 2.

Table 2. Measurement Data of Camera 1 and Manipulator.

No. of screw hole (Unit)	X_C *(pixel)*	Y_C *(pixel)*	X_A *(mm)*	Y_A *(mm)*
1	1189	557	430.16	59.21
2	989	507	425.38	39.62
3	783	509	426.36	20.84
4	571	675	441.12	0.58
5	53	301	406.43	-47.29
6	161	251	402.62	-39.09

Calculation

Substituting the 6 data shown in Table 2 into Eq. (13), we can obtain:

$$\begin{bmatrix} X_{C1} & Y_{C1} & 1 \\ X_{C2} & Y_{C2} & 1 \\ \vdots & \vdots & 1 \\ X_{C6} & Y_{C6} & 1 \end{bmatrix} = \begin{bmatrix} r_{11} \\ r_{12} \\ X_0 \end{bmatrix} = \begin{bmatrix} X_{A1} \\ X_{A2} \\ \vdots \\ X_{A6} \end{bmatrix}. \tag{14}$$

$$\begin{bmatrix} X_{C1} & Y_{C1} & 1 \\ X_{C2} & Y_{C2} & 1 \\ M & M & 1 \\ X_{C6} & Y_{C6} & 1 \end{bmatrix} \begin{bmatrix} r_{21} \\ r_{22} \\ Y_0 \end{bmatrix} = \begin{bmatrix} Y_{A1} \\ Y_{A1} \\ M \\ Y_{A6} \end{bmatrix}. \tag{15}$$

Equations (14) and (15) can be simplified as:

$$C \begin{bmatrix} r_{11} \\ r_{12} \\ X_0 \end{bmatrix} = A_X, \tag{16}$$

$$C \begin{bmatrix} r_{21} \\ r_{22} \\ Y_0 \end{bmatrix} = A_Y, \tag{17}$$

where C denotes the matrix of data, and A_X, A_Y denote the X, Y coordinate value for manipulator respectively. The value of transformation matrix T can be solved as:

$$T = \begin{bmatrix} r_{11} & r_{12} & X_0 \\ r_{21} & r_{22} & Y_0 \\ 0 & 0 & 1 \end{bmatrix} = \begin{bmatrix} -0.0001 & 0.0916 & 379.2838 \\ 0.0940 & 0.0012 & -53.6209 \\ 0 & 0 & 1 \end{bmatrix}. \tag{18}$$

The r_{12} is not equal to r_{21}, which is due to the existence of measurement errors of data (X_A, Y_A) and (X_C, Y_C).

After obtaining the transformation matrix T, the coordinate value (X_A, Y_A) of any screw hole can be solved by image processing even though the cellphone is randomly moved.

FINE TUNING ALGORITHM DEVELOPED BY CAMERA 2

Fine tuning algorithm is developed by manually operating the manipulator to align the screw with a screw hole and using camera 2 to take picture of the screw hole closely at the fixed height. The image coordinate value of the center of the screw hole can be obtained by image processing. It should be noted that the center coordinate values will be the same for any screw hole if the screw is aligned with that screw hole and the picture is taken at the same height. Next, an error correction equation is developed by horizontally moving the manipulator 1 mm forward, backward, left, right and take pictures at these positions as shown in Figure 20 respectively.

Fig. 20. Five pictures taken by camera 2.

The corresponding coordinate values obtained by image processing are shown in Table 3, where (x, y) denotes the deviation of the manipulator to the hole center position, and (X_C, Y_C) the image coordinate value of the center hole position with respect to the camera 2, and (X_D, Y_D) the image deviation value of the hole center position.

The error correction equation can be written as:

$$\begin{bmatrix} x \\ y \end{bmatrix} = \begin{bmatrix} a & b \\ c & d \end{bmatrix} \begin{bmatrix} X_D \\ Y_D \end{bmatrix}, \qquad (19)$$

where (a, b, c, d) denote the ratio parameters of hole position error to image deviation value of the hole center. These four unknowns are required to be solved. With this approach, we can improve the repeatability of our manipulator, which is originally ± 0.02mm.

Calculation

Substituting the data in Table 3 into Eq. (19) gives

$$\begin{bmatrix} a & b \\ c & d \end{bmatrix} = \begin{bmatrix} -0.00552 & 0.02438 \\ 0.02169 & -0.00327 \end{bmatrix}. \qquad (20)$$

Table 3. Measurement Data of No. 6 Screw Hole.

Position (Unit)	X_A (mm)	Y_A (mm)	x (mm)	y (mm)	X_C (pixel)	Y_C (pixel)	X_D (pixel)	Y_D (pixel)
Aligned	402.42	-39.60	0	0	289	133	0	0
1mm forward	403.42	-39.60	1	0	285	93	-4	-40
1mm backward	401.42	-39.60	-1	0	297	173	8	40
1mm right	402.42	-38.61	0	1	247	143	-42	10
1 mm left	402.42	-40.59	0	-1	335	123	46	-10

During screw tightening process, the end effector of the manipulator is driven to align the screw with the target hole at predetermined height and attitude. A close-up snap-shot is taken by camera 2 to obtain the image deviation value (X_D, Y_D). By applying the error correction equation (19), we can fine tune the end effector position and perform screw tightening precisely.

THE PROCESS OF THE PROGRAM AND EXPERIMENT

The flow chart for the whole system is shown in Figure 21. The whole process is divided into calibration step and screw tightening step. Calibration step is only processed once in advance.

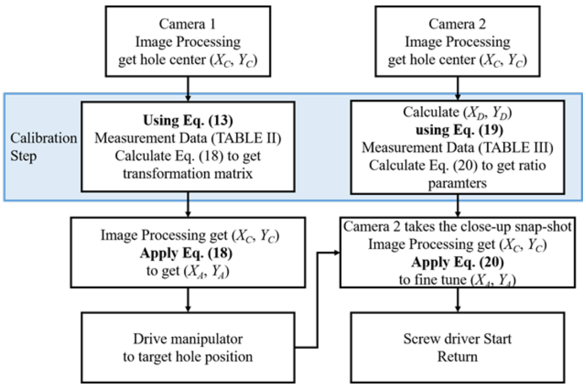

Fig. 21. The flow chart illustrates the whole process.

Due to the large number of cellphone screw holes, and the body image of the cellphone is complex. In order to speed up the image processing, only the screw holes to be tightened are numbered and processed.

The process of tightening screw and its results are illustrated as follows:

1. Click the "Detect1" button in HMI.
2. Read the image captured by the camera 1 (Figure 22a).
3. Perform hole selection (Figure 22b to c),
4. Perform color model conversion (Figure 22d).
5. Apply Gaussian filter, erode, dilate (Figure 23e), adaptive threshold (Figure 23f), Canny edge

detection (Figure 23g), and Hough circle detection (Figure 23h). The detected screw hole information is displayed on the HMI. Choose No.5 to tighten. HMI display screen is as shown in Figure 24.

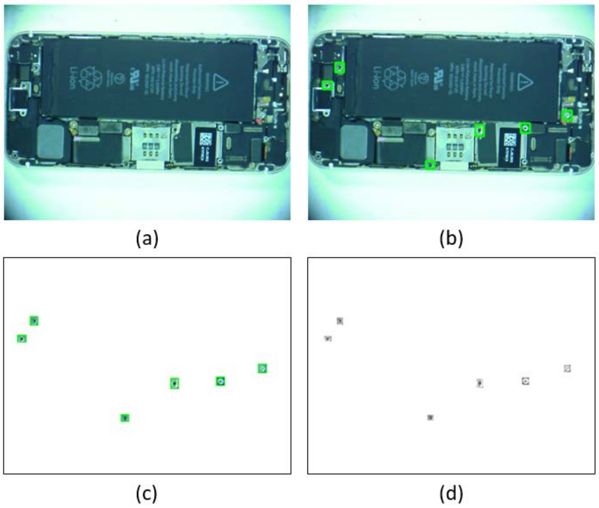

Fig. 22. (a) The original image taken by the camera 1. (b) Screw hole selection process. (c) The image after selecting the screw hole. (d) H single channel image.

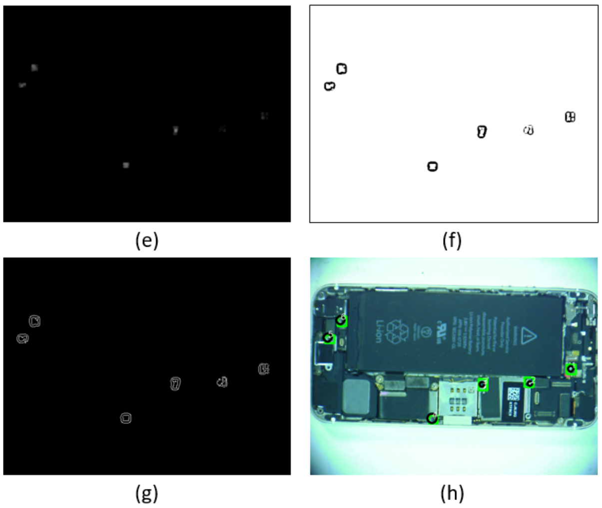

Fig. 23. (e) Image processed by Gaussian filter, erode and dilate. (f) Image processed by adaptive thresholding. (g) Image processed by Canny edge detection. (h) Image processed by Hough circle detection.

6. Click the "Detect2" button in HMI.
7. Read the image captured by the camera 2 (Figure 25i).
8. Perform color model conversion (Figure 25j), median filter, erode, dilate (Figure 25k), adaptive threshold (Figure 25l), four connected components (Figure 26m), Canny edge detection (Figure 26n), Hough circle detection (Figure 26o), and final image after process (Figure 26p). The detected screw hole information is displayed on the HMI as shown in Figure 27.

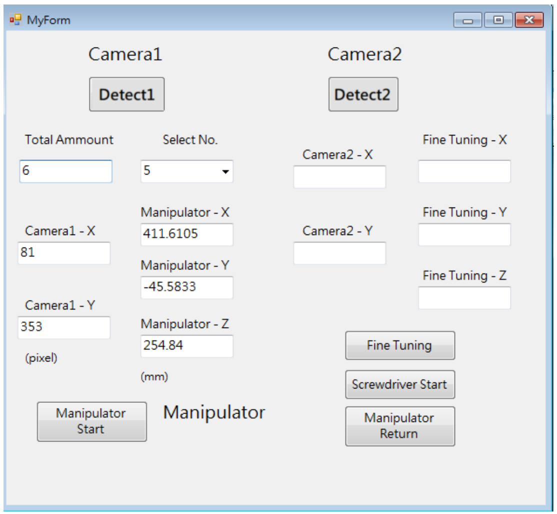

Fig. 24. HMI in initial positioning control.

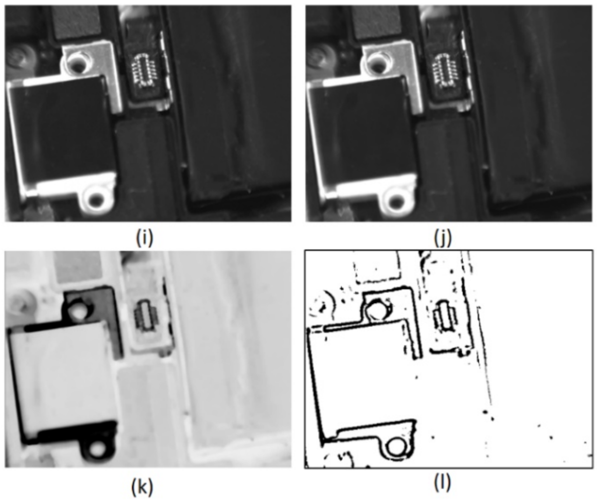

Fig. 25. (i) The original image taken by the camera 2. (j) H single channel image(k) Image processed by median filter, erode and dilate (l) Image processed by adaptive thresholding

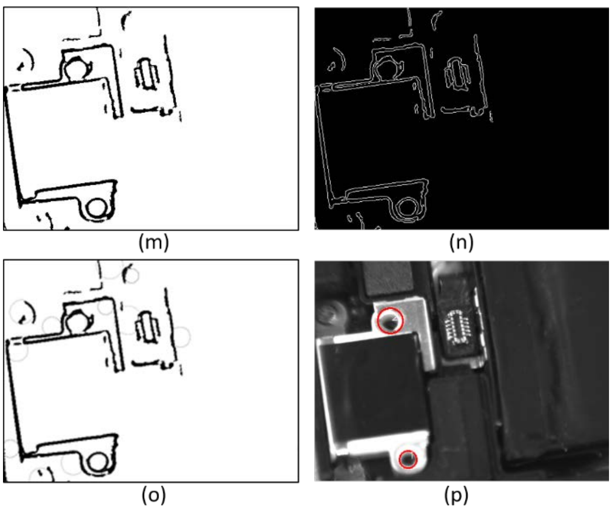

Fig. 26. (m) Image processed by four connected components. (n) Image processed by Canny edge

detection. (o) Image processed by Hough circle detection. (p) Final image after process

9. Click the "Fine Tuning" button to fine-tune the manipulator and move it to target position as shown in Figure 28.
10. Click the "Screwdriver Start" button to perform screw tightening (Figure 29).
11. Click the "Manipulator Return" button (Figure 30).

It should be noted that above process can be automatically performed without clicking the buttons.

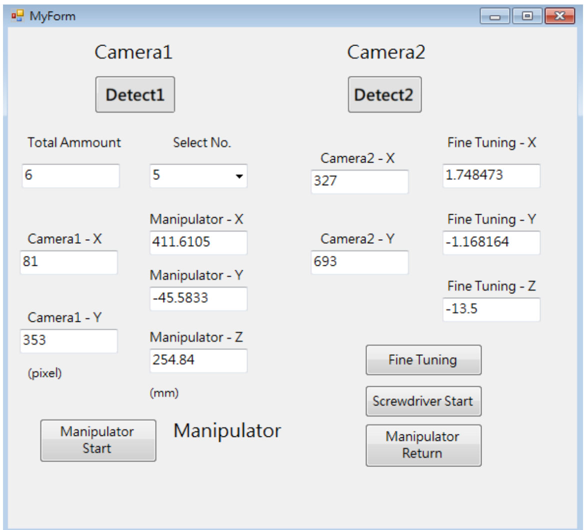

Fig. 27. HMI in fine positioning control.

Fig. 28. Manipulator is fine-tuned.

Fig. 29. Screw tightened completely.

Fig. 30. Manipulator return.

CONCLUSION

A fine-tuning algorithm is developed to enhance the accuracy of detection of hole position of the cellphone. Experimental results show that the proposed fine-tuning algorithm can tighten M1 screws into the target holes with the manipulator. Image processing developed in this study takes about 1 second to detect the coordinate value of the hole center. It takes 5 seconds for positioning and screw tightening if the robotic manipulator moves slowly and 2 seconds for fast moving. It is noted that an industrial personal computer having AMD Athlon 64 × 2 CPU of 21 GHz clock rate is used to perform image processing.

Approximate success rate is obtained by performing the experiment several times. For image processing, the success rate of detection of screw holes in the initial positioning was 95% or more. The main reason for failure was the mistake in selecting the screw hole. The success rate of fine positioning control detection is 90%. The main reason for this failure is the change in the light source after the cellphone is moved. For actual tightening, the success rate of M1.1 is 80%, and that of M1 is about 60%. The main reason for this is that M1 screws are much shorter. It is difficult to determine the angular accuracy of the screw on the screwdriver head since the screw is installed to screw driver head manually and stuck to it by magnetic force. A slight offset in angular direction causes failure. In the future, automatic screw feeder machines can be introduced to reduce the instability of manual mounting screws, and increasing the success rate thereby. Since there are no researches related to tighten tiny screws in recent years, this paper does not provide performance comparison with other studies.

REFERENCES

AhYin, X.Y., "Operators to Dilate and Erode Color impulse noise Images Based on the Morphology," *International Conference on E-Business and E-Government*, pp.4286-4288 (2011).

Ballard, D.H., "Generalizing the Hough Transform to Detect Arbitrary Shapes," *Pattern Recognition*, Vol. 13, No. 2, pp.111-122 (1981).

Bergen, J.R., Shvaytser, H., "A probabilistic algorithm for computing Hough transforms," *Journal of Algorithms*, Vol. 12, No. 4, pp.639-656 (1991).

Bliton, A.C., Patton, M.J., Rolli, M. L., "Microscopic motion analysis: Laplacian-of-Gaussian masks for subpixel edge detection," *Proceedings of the Annual International Conference of the IEEE Engineering in Medicine and Biology Society*, pp.1098-1099 (1988).

Bora, D.J., Gupta, A.K., Khan, F. A., "Comparing the Performance of L*A*B* and HSV Color Spaces with Respect to Color Image Segmentation," *International Journal of Emerging Technology and Advanced Engineering*, Vol. 5, No. 2, pp.192-203 (2015).

Chen, T. C., Chung, K. L., "An efficient randomized algorithm for detecting circles," *Computer Vision and Image Understand*, Vol.83, No. 2, pp.118-124 (2000).

Craig, J.J., *Introduction to Robotics – Mechanics and Control* (3rd Edition), Pearson Education, London, pp.19-61 (2008).

Gonzalez, R.C., Woods, R.E., *Digital Image Processing* (3rd Edition), Pearson Education, London, pp.795-860 (2007).

Jain, R.K., Majumder, S., Dutta, A., "SCARA based peg-in-hole assembly using compliant IPMC micro gripper," *Robotics and Autonomous Systems*, Vol. 61, No. 3, pp.297-311 (2013).

Ma, Z.X., Zhu, J., Li, W., "Detection of Point Sources in X-ray Astronomical Images Using Elliptical Gaussian Filters," *International Conference on Image, Vision and Computing*, pp.36-40 (2017).

Nnolim, U.A., "An adaptive RGB colour enhancement formulation for logarithmic image processing-based algorithms," *Optik*, Vol. 154, pp.192-215 (2018).

Pérez, L., Rodríguez, Í., Rodríguez, N., "Robot Guidance Using Machine Vision Techniques in Industrial Environments: A Comparative Review," *Sensors*, Vol. 16, No. 3, pp.335 (2016).

Pitipong, S., Pornjit, P., Watcharin, P., "An automated four-DOF robot screw fastening using visual servo," *IEEE/SICE International Symposium on System Integration*, pp.379-383 (2010).

Sharmila, B.S., Kaulgud, N., "Comparison of time complexity in Median Filtering on Multi-core Architecture," *International Conference on Advances in Computing,Communication & Automation*, pp.209-212 (2017).

Tzvi, D.B., Sandler, M.B., "A Combinatorial Hough Transform," *Pattern Recognition Letters*, Vol. 11, No. 3, pp.167-174 (1990).

工業機器人應用於手機微小螺絲自動鎖附之實現

呂睿晨 董必正
國立中央大學機械工程學系

李安謙
國立交通大學機械工程學系

摘 要

本研究目的主要是透過六軸機械手臂自動鎖附細小螺絲於手機。架構為機械手臂與兩個CCD攝影機配合，分別執行初始定位控制及精密定位控制。其中，一個攝影機固定在螺絲孔上方的固定架上，另一個則安裝在機械手臂末端的執行器上。方法為將獲取的影像進行影像處理及分析，以檢測螺絲孔的座標位置，並且利用座標轉換，找到孔的空間座標位置，開發一種微調演算法以提高孔座標的檢測精度。實驗結果驗證，所提出的微調演算法可以藉由機械手臂將M1和M1.1螺絲鎖附到目標孔中。